Science of the Total Environment 953 (2024) 176009

Contents lists available at ScienceDirect

Science of the Total Environment

journal homepage: www.elsevier.com/locate/scitotenv

Quantitative analysis of microplastics in beach sand via low-temperature solvent extraction and thermal degradation: Effects of particle size and sample depth

Mythreyi Sivaraman, Lingfei Fan, Weile Yan *

Department of Civil and Environmental Engineering, University of Massachusetts Lowell, MA, United States

HIGHLIGHTS

- Room-temperature solvent extraction followed by Py-GC-MS enabled facile and sensitive detection of PET and PS in beach sand;
- A majority of PET and PS debris identified were smaller than 100 microns, and they were more enriched in the top 5 centimeters of the beach sand;
- Results support the notion that beaches are important sites of microplastic formation.

GRAPHICAL ABSTRACT

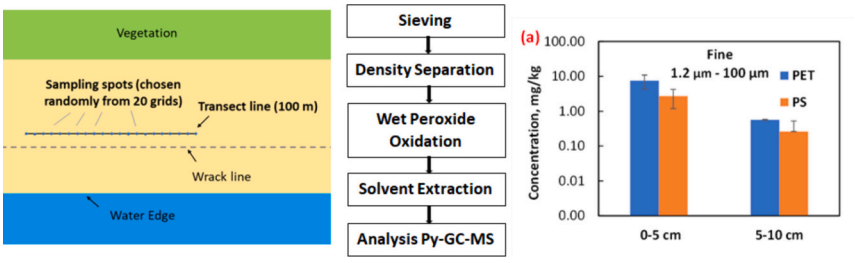

ARTICLE INFO

Editor: Damia Barcelo

Keywords:
Microplastics
Degradation
Fragmentation
Pyrolysis
Py-GC–MS
Solvent extraction
Beach sampling

ABSTRACT

Quantifying trace levels of microplastics in complex environmental media remains a challenge. In this study, an approach combining field collection of samples from different depths, sample size fractionation, and plastic quantification via pyrolysis-gas chromatography–mass spectrometry (Py-GC–MS) was employed to identify and quantify microplastics at two public beaches along the northeast coast of the U.S. (Salisbury beach, MA and Hampton beach, NH). A simple sampling tool was used to collect beach sand from depth intervals of 0–5 cm and 5–10 cm, respectively. The samples were sieved to give three size fractions: coarse (>1.2 mm), intermediate (100 μm–1.2 mm), and fine (1.2 μm–100 μm) particles. Following density separation and wet peroxide oxidation, a low-temperature solvent extraction protocol involving 2-chlorophenol was used to extract polyester (PET), polystyrene (PS), polyamide (PA), and polyvinyl chloride (PVC). The extract was analyzed using Py-GC–MS for the respective polymers, while the solid residue was pyrolyzed separately for polyethylene (PE) and polypropylene (PP). The one-step solvent extraction method significantly simplified the sample matrix and improved the sensitivity of analysis. Among the samples, PET was detected in greater quantities in the fine fraction than in the intermediate size fraction, and PET fine particles were located predominantly in the surface sand. Similar to PET, PS was detected at higher mass concentrations in the fine particles in most samples. These results underscore the importance of beach environment for plastic fragmentation, where a combination of factors including UV irradiation, mechanical abrasion, and water exposure promote plastic breakdown. Surface accumulation of fine plastic particles may also be attributed to transport of microplastics through wind and tides. The proposed sample treatment and analysis methods may allow sensitive and quantitative measurements of size or depth-related distribution patterns of microplastics in complex environmental media.

* Corresponding author.
E-mail address: weile_yan@uml.edu (W. Yan).

https://doi.org/10.1016/j.scitotenv.2024.176009
Received 24 May 2024; Received in revised form 14 August 2024; Accepted 1 September 2024
Available online 2 September 2024

1. Introduction

In recent years, there has been an increased awareness around plastic pollution due to high volumes of plastic usage and the ubiquitous presence of plastics in consumer products. Increased production along with low recycling rates and stable nature of plastic materials exacerbate the issue of plastic debris accumulation in the environment. In particular, micro- and nanoplastics (MNP), which are defined as plastic particles <5 mm and a micron respectively (GESAMP, 2016; Masura et al., 2015), have been detected in all regions across the world (Bergmann et al., 2019; Hale et al., 2020). MNP occurs ubiquitously in terrestrial, marine, and freshwater environments (Zhou et al., 2019) as well as water treatment systems (Murphy et al., 2016; Sun et al., 2019). Once released to the environment, plastics may undergo continuous chemical transformation, surface erosion, and fragmentation through interaction with sunlight, microbes, and chemical excipients found concurrently (Chamas et al., 2020; Gewert et al., 2015). Depending on the type of plastics and the environment they are found, photolytic and hydrolytic reactions are the main mechanisms of polymer degradation (Andrady, 2017; Gok et al., 2019). These processes result in the scission of polymer chains, change in crystallinity, and introduction of oxygenating groups that eventually lead to polymer embrittlement and fragmentation, giving rise to microplastics (Andrady, 2011).

Approximately 80 % of the plastic pollution in the marine environment is transported from terrestrial sources via rivers, wind, and beach littering (Kane et al., 2020; Lebreton et al., 2019; Lebreton et al., 2017). The transport of a plastic particle by water is a function of its size, shape, and density as these properties determine the minimum velocity required for its lateral transport and its vertical position in the aquatic environment (Browne et al., 2010; Egger et al., 2020; Li et al., 2020). Several studies on microplastics in shorelines have identified major types of consumer plastics including polyester (PET), polypropylene (PP), polyethylene (PE), polymethyl methacrylic (PMMA or acrylic), and polyamide (PA) fibers contaminating the coastal areas, especially in densely populated areas and environments that receive sewage or wastewater treatment effluent (Browne et al., 2011; Thompson et al., 2004). Beaches can become hotspots for plastic litter due to their proximity to urban centers or high levels of tourism activities. Additionally, beaches may serve as an important venue for plastic weathering (Andrady, 2017). Studies have examined the distribution of microplastics in the beach environment based on the landscape and depth of sampling (Piperagkas et al., 2019; Wessel et al., 2016) as well as the influence of seasonal events (Alvarez-Zeferino et al., 2020; Piperagkas et al., 2019) and anthropogenic activities (Retama et al., 2016; Tiwari et al., 2019) on microplastic occurrence. Most of the studies relied on identification of microplastics via direct visual or microscopic inspection, and the pollutants are quantified by item counts. However, this approach poses a challenge for detecting plastics of very small sizes. Partly for this reason, fewer studies have examined the size-dependent distribution of microplastics in beach environment down to sub-mm sizes. Such information, if available, can provide insights into plastic weathering and fragmentation processes occurring in the beach ecosystem.

In plastic weathering studies, pre-manufactured plastic materials (e.g. pellets or coupons) were often employed, and aging was conducted under laboratory or simulated field conditions. To properly interpret the laboratory weathering data, direct observation of degradation and transport of native plastic pollutants in the natural environment is necessary. However, analysis of microplastics in environmental samples is challenging due to their low abundance amidst the background of inorganic solids, natural organic matter, and other debris (Conley et al., 2019; Steinmetz et al., 2020). Pretreatment methods are commonly used to facilitate the extraction of microplastics from their original matrices, thereby improving the sensitivity and accuracy of microplastic identification. It is common to employ a cascade of pretreatment steps including density separation for reducing inorganic background constituents (Quinn et al., 2017), wet peroxide oxidation to remove background natural organic matter (Fischer and Scholz-Böttcher, 2017), and enzymatic digestion to partially eliminate natural polymers (Simon et al., 2018). Microplastics in the residual after pretreatment are detected via visual and microscopic inspection based on their physical appearance. More recently, thermo-analytical methods capable of identifying and quantifying mass abundances of polymers have gained significant interest (Becker et al., 2020; Fischer and Scholz-Böttcher, 2019; Peñalver et al., 2019). Thermo-analytical techniques include thermogravimetric analysis (TGA, often hyphened with mass spectrometry or other analytical techniques), thermal desorption-gas chromatography–mass spectrometry (TED-GC–MS), and pyrolysis-gas chromatography–mass spectrometry (Py-GC–MS). These methods are subject to less interference from environmental matrices (Becker et al., 2020; Seeley and Lynch, 2023; Steinmetz et al., 2020). Among them, Py-GC–MS is the most common thermo-analytical method for microplastics research because of its sensitivity and specificity. The pyrolysis step of the analysis can convert polymers into low molecular-weight fragments. Separation, identification, and quantification of characteristic fragments by GC–MS reveal the identity and mass of polymers present in the original sample (Fischer and Scholz-Böttcher, 2017, 2019; Käppler et al., 2018). Recent progress in Py-GC–MS method development advocates the use of a double-shot pyrolysis mode for samples with background organics, as an initial thermal desorption step helps to eliminate volatile organics prior to pyrolysis, thereby significantly improving analysis sensitivity (La Nasa et al., 2020; Okoffo et al., 2020). Additionally, the ability to incorporate internal standards in thermal analytical methods further strengthens the quality of analysis (David et al., 2018; Fischer and Scholz-Böttcher, 2019).

In most of the studies that employ Py-GC–MS, microplastics were analyzed in solid particle form. This approach is affected by the sample size limit of the pyrolysis instrument, non-uniform selection of pyrolysis material from the parent sample, and the availability of standards of small but accurate masses. In recent studies, solvents have been used for plastic extraction. Solvents such as 1,2,4-trichlorobenzene (1,2,4-TCB) and dichloromethane (DCM) were used to extract mainly polystyrene (PS) (Ceccarini et al., 2018; Steinmetz et al., 2020). Pressurized liquid extraction (Okoffo et al., 2020) or microwave-assisted extraction (La Nasa et al., 2020) was used to improve DCM extraction efficiency of PS, PMMA, and various plasticizers, but these methods are not effective for other common plastics such as PET. Studies have explored sequential steps of solvent extraction employing DCM and tetrahydrofuran (THF) for extracting PS, polyvinyl chloride (PVC), PMMA and ABS copolymers, and hexafluoroisopropanol (HFIP) for Nylon 6 (or PA-6), Nylon 6,6 (or PA-66), and PET (Matsueda et al., 2021). However, the procedure involved is complex and may introduce interference for quantitation.

This study aims at bridging the gaps in the current microplastic sampling and analysis methods by developing a simple beach sampling method and streamlined sample pretreatment and thermal analysis protocols to enable systematic examination of the effects of particle size and sampling depth on the distribution of common consumer plastics in the beach environment. Specifically, samples were collected at two popular beaches in Massachusetts and New Hampshire, United States using a facile sampling method for rapid collection of surficial and subsurface sand. After size fractionation and pretreatments to remove background materials, a new low-temperature solvent-extraction technique coupled with Py-GC–MS analysis was applied to obtain sensitive and robust quantitation of a variety of plastic types of common occurrence. The implications of the observed size and depth-dependent distribution of plastics in terms of the formation and migration of microplastics in natural systems are then discussed.

2. Materials and methods

2.1. Chemicals and reference standards

All chemicals used were of ACS reagent grade or higher. Reference standards of PET, PS, PA-66 (or Nylon 6,6), and PVC were from Polymer Kit 1.0 from Hawaii Pacific University. PE microspheres (212–250 μm, Cospheric, CA) and commercial PP fishing rope were used to prepare PE and PP standards for calibration of the thermal analysis method. The pyrolysis products of the PP rope were identical to those of the PP reference in Polymer Kit 1.0, and the rope was used instead of PP beads in the kit for the ability to obtain very thin strands of desired lengths. Deuterated PS (P40556, Polymer Source Inc., Canada) dissolved in DCM was used as an internal standard. All materials were handled with metal tools and stored in metal or glass containers. Contact with clothing made of synthetic fibers was avoided during field sampling, sample processing, and instrument analysis.

2.2. Field sampling

Beach sand samples were collected at Salisbury Beach in MA and Hampton Beach in NH in Jun 2021. The two public beaches are approximately 5 miles apart (Fig. 1a). Hampton Beach is a well-developed tourist site with a significant concentration of commercial entities along the beach. There are several fisheries around the Hampton Beach State Park, located ca. 1 mile to the south of the beach. The sampling site of Salisbury Beach sits on Salisbury Beach State Reservation and is close to the southern end of the shore where the Merrimack River enters the Atlantic. Sampling procedures were adapted from existing beach sample protocols developed by the NOAA, UNEP, and Rocha guidelines (Cheshire and Adler, 2009; Lippiatt et al., 2013; Sluka et al., 2018). Information on tidal activity for both beaches was gathered to help determine the wrack line. The wrack line is an area on the beach where organic material and debris from the ocean, consisting typically of seagrasses, algae, mangrove leaves, propagules, and shells of crustaceans, are deposited at a high tide. Prior to sampling, the site was surveyed to record the distance from the wrack line to water edge and backend vegetation zone, the aspect, latitude, and longitude of the shoreline. After performing site characterization, 2 transects of 100 m each were chosen at each beach as shown in Fig. 1b. Each transect was parallel to the wrack line and was positioned 2–3 m away from the wrack line closer to the vegetation zone. This ensures sufficient distance both from water and vegetation and avoids areas of high human traffic, the latter typically occur in front of the wrack line. A transect was divided into 20 sections of 5 m each. Samples were collected from 4 sections at each transect. These sections were chosen using random numbers generated by a computer prior to the sampling activity. The randomly chosen sections were inspected visually, and any large surface debris that resembled plastics and was >2.5 cm was picked up manually. After this, a 20-cm diameter stainless steel ring, re-purposed from a cake ring, was placed at the midpoint of a section, and pressed into the sand until it reached a depth of 5 cm as indicated by a marking on the ring. The sand surrounding the ring was removed, and a stainless-steel plate was inserted underneath the ring to collect the top 5 cm layer of sand. Subsequently, the ring was pressed at the same spot to a depth of 10 cm to collect a sub-surface layer of sand (5–10 cm). This sampling method can in principle allow sampling at a greater depth, but for this initial study, samples were collected at two depth intervals up to 10 cm deep. The surface and subsurface sand was deposited into two steel buckets and the same procedure was repeated at all 8 sections of the 2 transects. The sand collected from the same depth interval at 8 sections of a beach was combined into one composite sample.

2.3. Sample pretreatment

Fig. 2 illustrates the pretreatment process flow used to prepare beach sand samples for thermal analysis. Samples were initially air dried for 24–48 h to remove moisture. The dried sand was mechanically sieved to divide into 3 size fractions: coarse (>1.2 mm), intermediate (100 μm–1.2 mm), and fine (1.2 μm–100 μm). For both beaches irrespective of sample depth, >85 % of the mass of the sample was in the intermediate size fraction. The fine fraction collected the smallest quantity (<1 %). The coarse fraction accounted for approximately 10 % of the mass. Due to the sensitivity of the Py-GC–MS instrument (plastics >50 μg may overwhelm the instrument), the coarse fraction was subjected to visual inspection and Fourier transform infrared spectroscopy (FTIR) analysis only. The intermediate and the fine fractions were subject to further processing as described below.

As the quantity of the fine fraction was small, the entire fraction went through pretreatment steps together until after wet peroxide oxidation, where the sample was split prior to undergoing solvent extraction. Since the intermediate fraction was a bulk quantity (>30 lbs), subsampling was required to reduce the quantity to facilitate better pretreatment. For the sub-sampling, the intermediate fraction was evenly spread on a large clean cardboard tray of ca. 0.5 × 1.5 m in size. The tray was divided into 12 sections of equal size, and 4 sections were chosen randomly wherein a 15 cm × 15 cm square-shaped stainless steel cake ring was used to collect the sand material within the ring. The mass of the subsample collected in each section was approximately 200–300 g, which was combined before being split into triplicates. This approach ensured that the subsamples are representative of the original sample.

The pretreatment steps were designed based on the protocols described in the existing literature (Masura et al., 2015) with adaptations as suggested by preliminary trials performed on the intermediate fraction of the Salisbury Beach sample. Density separation was chosen as the first step of sample pretreatment, since it could significantly reduce the quantity of sample that should be further processed, thereby reducing chemical consumption in the subsequent wet peroxide oxidation and solvent extraction steps. After experimenting with sodium chloride, sodium metatungstate, and zinc chloride, zinc chloride at a density of 1.6 g/cm^3 was chosen for density separation due to its lower toxicity than sodium metatungstate and higher density than sodium chloride at an equivalent concentration (Coppock et al., 2017). To achieve the required density, 972 g of zinc chloride was added in 1 L of deionized water. 1 L of $ZnCl_2$ solution can process up to ca. 300 g of a sample. After mixing the sample with the salt solution, the slurry was set aside for a settling time of 3 h for the fine fraction samples and 1 h for the intermedium fraction. At the end of the settling time, the top portion of the solution containing the floating particles passed through a piece of glass microfiber filter (Whatman GF/C, 1.2 μm), where the particles were retained on the filter paper. The remainder of the solution was discarded. The collected particles were rinsed with DDI and dried at 105 °C for 24 h and 72 h, respectively, for the intermediate and fine fractions. To save chemical consumption, the spent zinc chloride solution was filtered through 1.2 μm glass microfiber paper twice and the filtrate was collected for reuse until the color of the solution darkened.

Following density separation, wet peroxide oxidation was performed to remove background organic matter. Samples were treated with Fenton's reagent (0.05 M Fe(II) + 30 % H_2O_2) at 75 °C for 30 min, after which the mixture was left aside for up to 48 h. The volume of the reagent solution used scaled with the quantity of the sample. For instance, samples in the range of 0.5–1.0 g required the use of 50 mL of Fenton's reagent. At the end of the digestion period, samples were filtered, and the solids collected were dried in the oven for 24 h at 105 °C.

Subsequently, the dried samples were extracted with 2-chlorophenol at room temperature for up to 48 h. Different solvents were tested to evaluate the dissolution of polymers. The details can be found in Table 1. 2-Chlorophenol was selected as the best solvent for its ability to dissolve PET, PS, PA-66, and PVC. Lab assessment indicates that PP and PE are not soluble in 2-chlorophenol, and they remained as solid residue during solvent extraction. The volume of solvent used to extract a sample depends on the sample quantity. 50 mL of 2-chlorophenol was appropriate

(a)

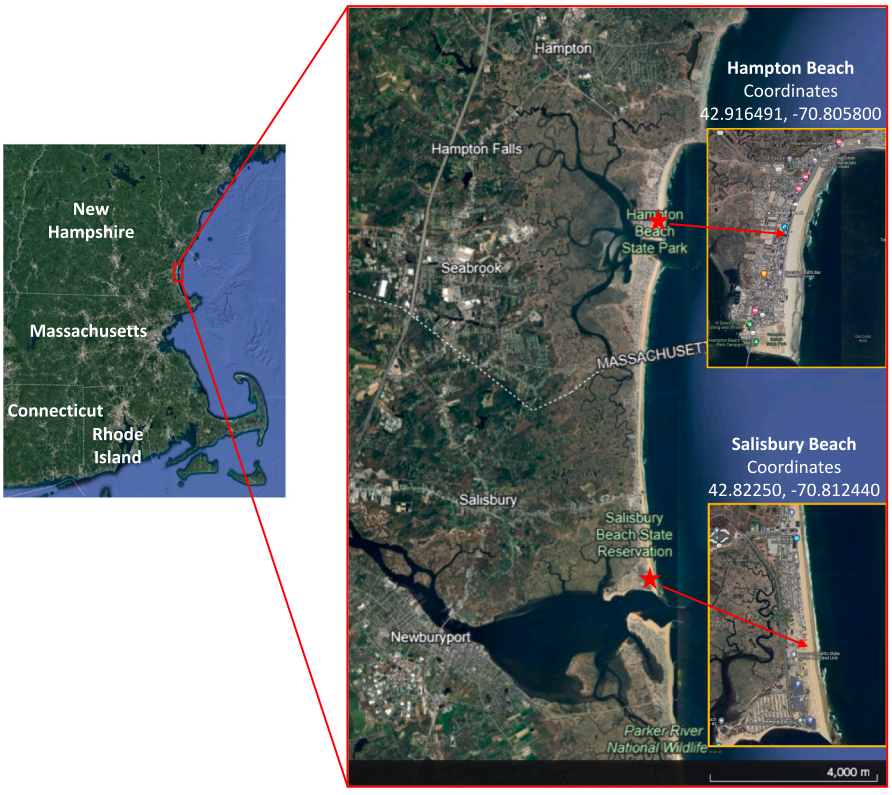

(b)

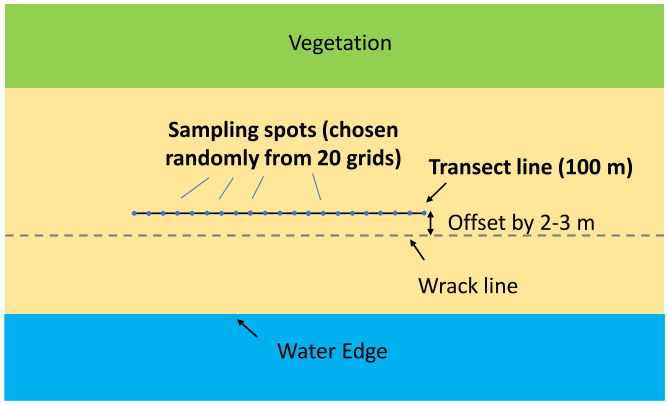

(c)

Fig. 1. (a) Map of sampling locations. (b) Schematic of sampling spots on the beaches. (c) Photo of a stainless-steel tool kit for surface and subsurface sample collection. Map imagery was obtained from Google.com.

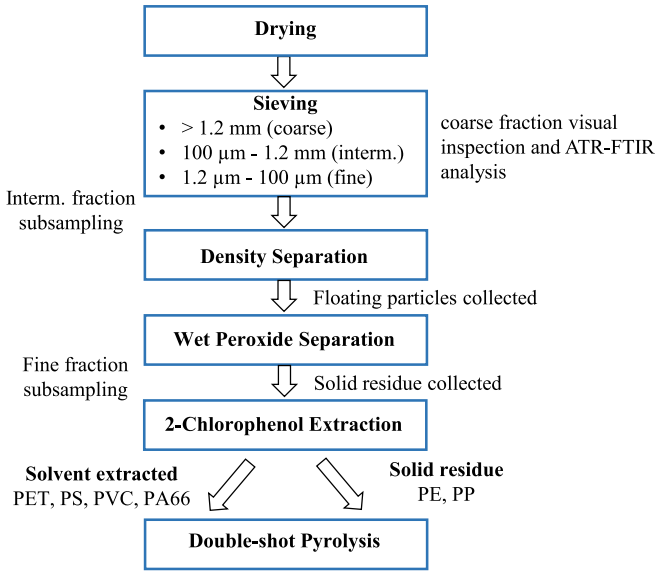

Fig. 2. Pretreatment process flow of beach sand.

Table 1
Density and solubility of common plastics in various solvents.

Type of plastics	Solubility in solvents at room temperature[a]		
	Acetone	Dichloromethane	2-Chlorophenol
LDPE/HDPE	N.S.	N.S.	N.S.
PP	N.S.	N.S.	N.S.
PET	N.S.	N.S.	Soluble
PS	N.S.	Soluble	Soluble
PVC	N.S.	N.S.	Soluble
PA-66	N.S.	N.S.	Soluble

[a] N.S. is not soluble.

for 0.5–1.0 g of solids. After the extraction period, the extract and the solid residue of a sample were separated by vacuum filtration using 1.2 µm glass microfiber paper. A small aliquot (50–150 µL) of the extract was transferred to a pyrolysis sample cup, where the solvent was driven off by heating the sample in a fume hood at ~165 °C for 0.5–1 h. The solid residue was directly transferred to a sample cup without any pre-heating. Except for PS analysis which was not amended with an internal standard (IS) due to potential interference, all samples were spiked with 10 µL of 10 mg/L deuterated polystyrene (d5-PS, Polymer Source Inc) in DCM as an IS prior to Py-GC–MS analysis.

2.4. Py-GC–MS analysis

The solvent extracted portion of a sample was analyzed by Py-GC–MS to identify PET, PS, PA-66 and PVC. The solid residue was analyzed for PE and PP. Py-GC–MS was performed in a micro-furnace pyrolyzer (EGA/PY-3030D, Frontier Lab, Japan) installed on a GC–MS system (Agilent 8890 GC-5977 MS) equipped with an Agilent HP-5 MS UI column (0.25 µm × 0.25 mm × 30 m) and an FID detector. The double-shot pyrolysis mode was used, and the method consists of an initial step of thermal desorption at a starting temperature of 100 °C, a ramp rate of 20 °C/min, and holding for 7.5 min at 250 °C. FID signals were acquired at this stage to determine sample cleanliness. The second shot (i.e., the pyrolysis step) was performed at 550 °C for 0.2 min. The pyrolysates were injected into the GC at a split ratio of 100:1 at an inlet temperature of 250 °C. The oven temperature ran from 70 °C to 320 °C at 20 °C/min and was held at 320 °C for 5 min. MS signals were acquired in scan and SIM modes and the abundance of quantifier ions of a characteristic product in the SIM mode was used to quantify the respective plastics. Each sample analysis was performed after two blank runs to ensure a clean background. Instrument calibration for each polymer type was carried out by analysis of the respective standards. The standards of PET, PS, PA-66, and PVC were prepared by dissolving known quantities of the respective reference materials in 2-chlorophenol. An appropriate aliquot of a standard solution and 10 µL d5-PS IS were deposited into a pyrolysis sample cup. As PE and PP were insoluble in 2-chlorophenol or other solvents evaluated (Table 1), PE and PP were calibrated by direct pyrolysis of a known quantity of the reference material. For PE, one to ten 250-µm spherical beads were used for calibration. As the beads were uniform in size, they were assumed to have similar mass. For PP, thin filaments of 1-cm length were used for calibration. The unit mass of one piece of the reference material was determined based on the mass of a collection of the reference material of a sufficient size (>10 mg) and the number of pieces in the collection.

3. Results and discussion

3.1. Minimization of background contamination

Since microplastics tend to be in minute quantities in environmental matrices, while plastic utensils and plastic-containing fabrics are ubiquitous in a laboratory environment, it was essential to control background contamination. In this study, leather gloves as well as metal buckets, trays, and hand tools were used during beach sampling. Clothing of synthetic fibers was avoided. Samples were stored in metal buckets covered with aluminum foil or in capped glass jars. In all laboratory pretreatment and analysis protocols, non-plastic containers and utensils were used. Glass microfiber filter papers were used to collect solid residue in a filtration procedure. Solvent extract was stored in glass vials. Prior to Py-GC–MS analysis, a small aliquot of solvent extract was transferred to a pyrolysis sample cup using a glass syringe. In our initial protocol, a sample cup was covered with a piece of perforated aluminum foil to avoid deposition of environmental debris into the sample cup during heating. However, a higher background in the resultant mass spectra suggests possible outgassing by the aluminum foil during heating. Given this, sample cups were covered with a glass beaker during heating, leaving a gap at the bottom to allow air circulation, which proved to introduce no additional background (refer to a photo of the setup in Fig. S3).

3.2. Method calibrations

During Py-GC–MS analysis, an IS is often used to account for variance in results due to changes in pyrolysis efficiency, matrix interferences with pyrolysis products, and variations in mass spectrometer sensitivity (Fischer and Scholz-Böttcher, 2019; Lauschke et al., 2021). Several ISs have been used by different groups, including small molecular compounds (e.g., cholanic acid), polycyclic aromatics such as anthracene, and deuterated polymers such as deuterated-polystyrene or polybutadiene (Becker et al., 2020; Fischer and Scholz-Böttcher, 2019). Polymer-based IS, especially deuterated polymers, are preferred because they behave more similarly to the plastic analytes during pyrolysis. Ideally, the polymer IS should be non-reactive with sample ingredients, have a unique quantifier that does not interfere with the identification and quantitation of sample pyrolysis products, and are of high-purity (Lauschke et al., 2021). However, limited choices of high-purity deuterated synthetic polymers are currently available for this purpose. Recent work has evaluated poly(styrene-d5), or d5-PS, and poly(4-fluorostyrene) as IS (Lauschke et al., 2021). Interference was observed due to interactions between d5-PS and the inorganic components of the sample matrix, which caused hydrogen-deuterium (H-D) exchange of the IS during pyrolysis, manifesting in a decrease in the intensity of the most abundant fragment of the IS (m/z 109), accompanied by an increase in the intensity of the adjacent fragment (m/z 108). The H-D exchange effect was most prominent in the presence of aluminum oxide

and sea sand, and it could lead to an overestimation of microplastics in samples (La Nasa et al., 2020). In this study, the concern over potential H-D exchange of IS was addressed by solvent extraction as it eliminates the inorganic matrix. Since poly(4-fluorostyrene) generates a fragment ion of *m/z* 122 in high abundance, which may interfere with PET analysis, it is not suitable for this study. Considering the above, d5-PS was used as the IS. Direct pyrolysis of d5-PS as a neat chemical indicates the presence of impurities, specifically a low level of undeuterated polystyene. To eliminate the interference effect of this impurity on polystyrene quantitation, calibration and sample analysis for PS were conducted without the amendment of IS in this study. As styrene monomer may be produced by natural organic matter such as chitin (Fischer and Scholz-Böttcher, 2019), styrene trimer signal at *m/z* 91 was used as the quantifier of PS in this study.

Our initial attempts for calibrating plastics using powder obtained from milling of coarse polymer beads or particles resulted in calibration data with poor linearity. Similar outcomes were observed when trying to establish Py-GC–MS calibrations using solid standards in prior studies (Fischer and Scholz-Böttcher, 2017, 2019). After careful evaluation of some common solvents as listed in Table 1 at different temperatures and dissolution durations, 2-chlorophenol was chosen as the solvent for extracting PET, PS, PVC, and PA-66. The choice of 2-chlorophenol proved prudent due to its ability to dissolve a variety of common consumer plastics, low volatility (boiling point at ca. 175 °C), low aqueous solubility, and high density (1.26 g/mL). Specifically, calibration standards were prepared from successive dilution of polymer extraction solution in 2-chlorophenol and subject to double-shot pyrolysis. Fig. 3 shows the calibration data of PET and PS, and those of PVC, and PA-66 are in Fig. S1. The GC–MS parameters used to quantify the respective polymer are summarized in Table 2. Using the solvent extraction method, robust calibration data of the four polymers were obtained. In the case of PET, linear responses of *m/z* 122 at a retention time of ca. 4.8 min normalized by the signal of IS was obtained with the mass of PET pyrolyzed in the range of 0.03–0.3 μg (Fig. 3a). For PS, an excellent calibration using *m/z* 91 at a retention time of ca. 11.8 min (no IS to minimize inference) was achieved with the mass range extended down to 0.02 μg (Fig. 3b). Similar to PET and PS, linear responses were obtained for PVC and PA-66 using the 2-chlorophenol extraction method. The quality-of-fit (r^2) was >0.99 for all calibrations.

In microplastic studies, a low level of detection (LOD) and level of quantitation (LOQ) are preferred, since microplastics are in significantly lower quantities against the background environmental matrices. These limits were determined based on replicate analysis of method blanks and low levels of standards and are defined as mass quantities that correspond to a signal-to-background-noise (S/N) ratio of 3 for LOD and 10 for LOQ, respectively (Fischer and Scholz-Böttcher, 2017; Okoffo et al., 2020). The LOQ values of the current analysis method are tabulated in Table 2. The instrument is capable of detecting minute quantities (<0.1 μg) of PET and PS. It is less sensitive to PA-66 (Fig. S1a) and PVC (Fig. S1b) due to relatively high backgrounds in the signals of interest in the method blanks. Sea biomass (e.g. chitin) and glass microfiber filter used seem to contribute to signals of PA-66 (Bour et al., 2018), while the indicator compound of PVC, benzene, may be generated at low levels by the solvent and natural organic matter in the samples. The method LOQs were calculated from instrument LOQs and the mass of samples processed by the pretreatment procedures. Samples of the intermediate size fraction have lower method LOQs than those of the fine fraction because a dominant proportion of a sample mass was within the intermediate size fraction and pretreatment such as density separation was able to remove a larger percentage of background materials from the intermediate-sized solids than the fine solids. Overall, compared to prior Py-GC–MS studies employing direct pyrolysis of polymers in a solid form, more robust calibration and lower quantitation limits are obtained by the solvent extraction method. The merits are mainly attributed to the method's ability to generate precise plastic standards at low concentrations and to prevent background matrix going into the pyrolyzer.

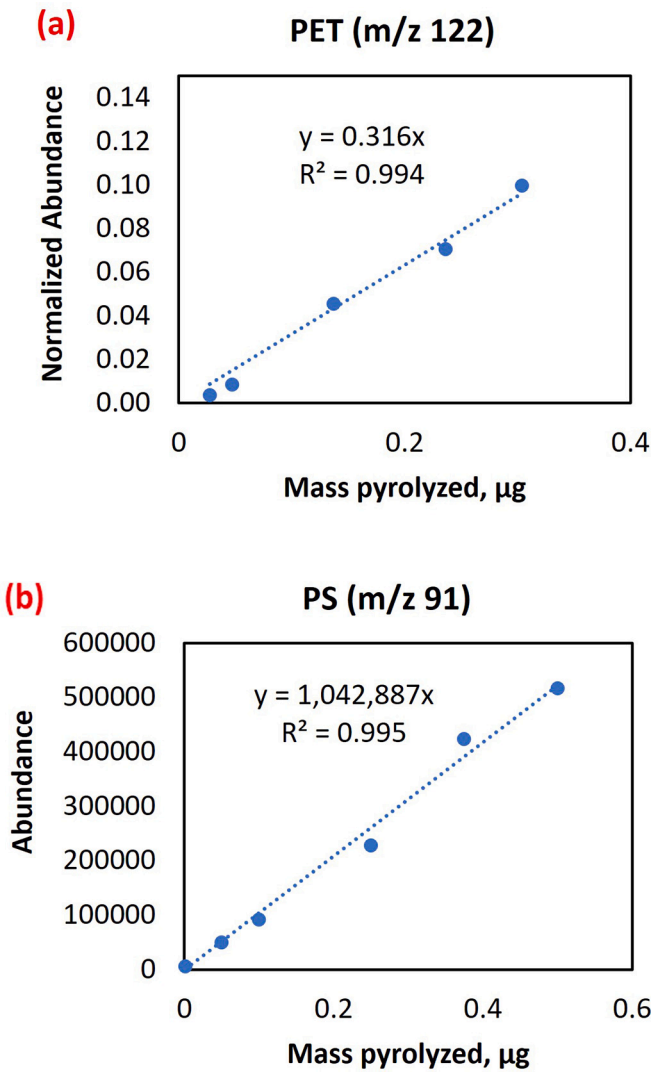

Fig. 3. Calibration results of (a) PET, (b) PS.

An additional advantage is related to the choice of the solvent. Compared to the solvents used in earlier studies including DCM, 1,2,4-TCB, THF, or HFIP (La Nasa et al., 2020; Matsueda et al., 2021; Okoffo et al., 2020) or the employment of sequential extraction using different solvents and acid/alkaline depolymerization (e.g., in PET hydrolysis) (Castelvetro et al., 2021), 2-chlorophenol is capable of dissolving a range of plastic materials. This eliminates the need for multiple rounds of extraction and simplifies sample pretreatment, which in turn reduces sample contamination and chemical usage. We also note that 2-chlorophenol is less volatile and has a more benign character than DCM used in prior studies (La Nasa et al., 2020; Matsueda et al., 2021). The latter is a volatile chemical with a boiling point of 39.6 °C and a probable carcinogen (OSHA), thus requiring additional safety precautions during sample handling.

PE and PP calibrations were performed on solid standards due to their negligible solubility in solvents (Table 1). In a previous study (Steinmetz et al., 2020), attempts were made at dissolving PE in 1,2,4-TCB at 120 °C for 4 h. Our trials using PE beads in the approx. size range of 40 μm to 1 mm show negligible solubility of PE in 1,2,4-TCB; therefore, direct pyrolysis of solid PE particles or PP fibers was performed. For quantitation, fragments of *m/z* 55 and 126 were chosen for PE and PP, respectively. The quality of the calibration lines (Fig. S2) was lower than that of the solvent extraction method, and this is constrained largely by the availability of solid standards of minute mass and the

Table 2
Characteristic products of common plastics during Py-GC-MS analysis.

Type of plastics	Characteristic products of Py-GC–MS				Instrument LOQ, μg	Method LOQ, mg/kg	
	Compound name	GC RT[a], min	MS qualifier	MS quantifier		Fine fraction	Intermediate fraction
PET	Benzoic acid/vinyl benzoate	4.8	77, 105, 122	122	3×10^{-2}	2	5×10^{-2}
PS	Styrene trimer	11.8	78, 91, 104	91	2×10^{-2}	1	3×10^{-2}
PA-66	N^1-(hex-5-enyl)-N^6-hexyladipamide	6.0	39, 55, 96	96	5	4×10^{2}	9
PVC	Benzene	2.2	78, 112	78	0.5	40	0.9
PE	1-Tetradecene	5.8	55, 69, 82, 83, 97	55	–	–	–
PP	2,4-Dimethyl-1-heptene	2.8	69, 70, 83, 111, 126	126	~1×10^{-2}[b]	–	–

[a] GC retention time.
[b] Based on extrapolation from the lowest standard.

accuracy of the analytical balance. In terms of LOQ, PP produces a strong and unique trimer fragment (*m/z* 126), whereas pyrolysis of PE generates alkanes and alkenes of varying chain-lengths that may also be found in background organics including adventitious hydrocarbons in air that tend to adhere to clean metal surfaces, a phenomenon well documented in the surface analysis field (Ramos et al., 2009). For this reason, the LOQ of PE was not determined. The determination of LOQ of PP involved a large degree of extrapolation from the lowest standard, since a smaller quantity cannot be reliably created for calibration. We therefore did not attempt to quantify the method LOQ.

3.3. Results of beach samples

PET and PS were identified in the solvent-extracted samples of both beaches. Nylon and PVC were not detected. In the analysis of replicate samples, an individual replicate with signals below LOQ was assigned a zero value and was included in the calculation of the average concentration of the sample. Fig. 4 shows the average concentrations of PET and PS in the fine and intermediate fractions, respectively, at Salisbury Beach. In the fine solids, the mass concentration of PET in the surface (0–5 cm) and subsurface (5–10 cm) sand is 6.0 ± 3.6 mg/kg and 0.35 ± 0.35 mg/kg, respectively. In the intermediate size fraction, PET debris was not detected in the surface sample, while PET concentration in the subsurface sample was 0.019 ± 0.03 mg/kg. Fine particulate PS was detected in the surface at 3.5 ± 0.3 mg/kg, and that in the subsurface was 2.2 ± 0.8 mg/kg. Compared to the fine solids, much smaller mass quantities of PS debris were identified in the intermediate size fraction, and their levels were comparable between the surface and subsurface depths (refer to data summary in Table S2). The levels of both PET and PS found at Salisbury Beach suggest a trend of increasing mass concentration as the particle size decreases, and this size-dependent change in mass distribution is more prominent for samples collected from the surface sand than the underneath layer.

The PET and PS data of Hampton Beach are summarized in Fig. 5. The average concentrations of PET in the fine fraction were found to be 7.6 ± 3.2 mg/kg and 0.57 ± 0.02 mg/kg in the surface 5 cm and 5 to 10 cm deep sand, respectively. PS debris in the same size fraction were at 2.7 ± 1.5 mg/kg in the surface sand, and 0.26 ± 0.26 mg/kg in the subsurface layer. Similar to Salisbury Beach, the amounts of PET found in the intermediate size fraction were approximately 1–2 orders of magnitude smaller than that in the fine fraction. In the case of PS, a higher quantity was detected in the 5–10 cm depth than the surface 5 cm in the intermediate-sized solids.

In all samples, neither PE nor PP could be detected above their LODs. Aside from high background interference of PE analysis, our limited ability to push the calibration ranges of PE and PP to low mass quantities is another reason for the relatively poor detection capability. Previous literature also indicated the issues of identifying PE and PP reliably in environment samples (Dümichen et al., 2017; Fischer and Scholz-Böttcher, 2017). Alternative analysis techniques, such as confocal or spectroscopic microscopy may be used in conjunction with Py-GC–MS in future analysis to identify these plastics with greater certainty. It was noted that the absolute abundance of signals used for quantitation of the IS was significantly lower for solid residue samples compared to the solvent extracted samples (Table S4), indicative of the occurrence of H-D exchange during solid residue analysis (Lauschke et al., 2021). This result shows that sample preparation via solvent extraction is advantageous to direct pyrolysis of solid samples by reducing matrix effects caused by background minerals.

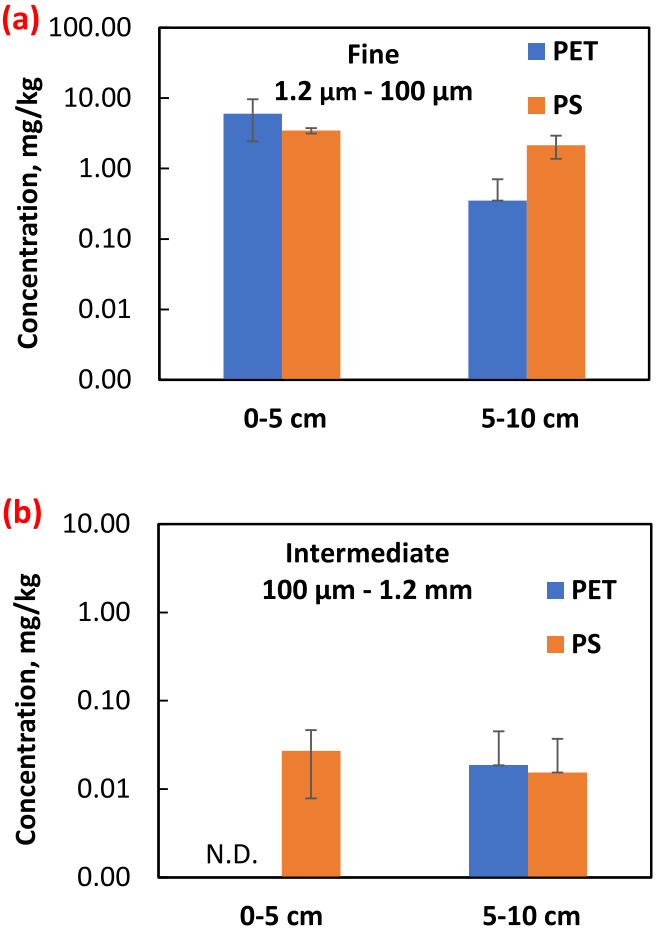

Fig. 4. Microplastics detected in different size fractions of (a) surface and (b) subsurface samples collected at Salisbury Beach.

3.4. Implications for plastic degradation

Across the samples, the observed mass concentration of plastics varies by several orders of magnitude, but similar trends can be identified in the results at both beaches, suggesting the existence of common processes controlling plastic distribution and degradation at the two beaches. Specifically, we noticed that the majority of the plastic debris in

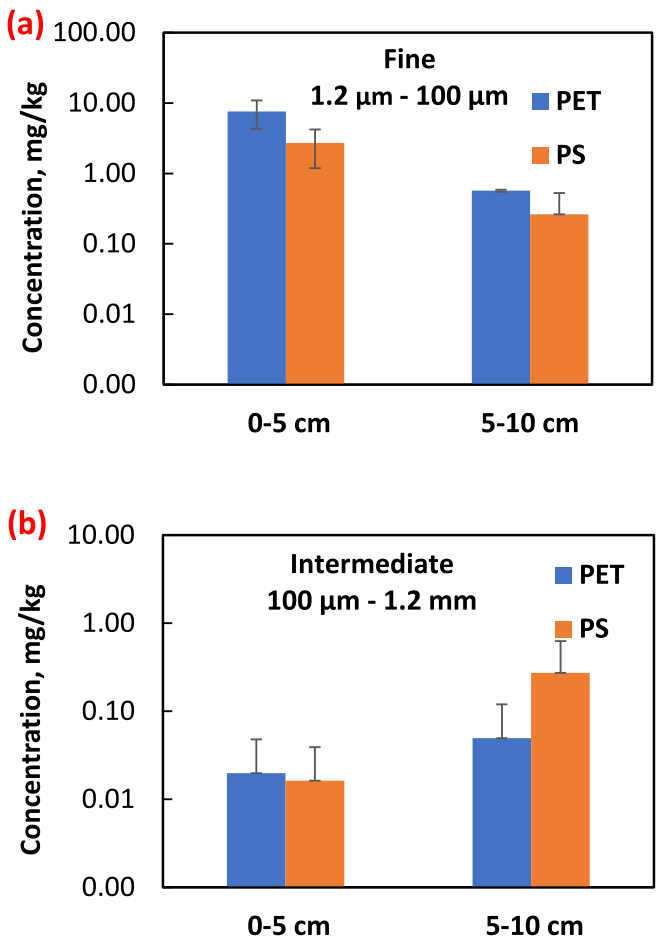

Fig. 5. Microplastics detected in different size fractions of (a) surface and (b) subsurface samples collected at Hampton Beach.

the two beaches consists of tiny particles <100 µm in size. The observation is consistent with a recent study that identified increasing mass quantities of plastics with smaller particle size in coastal sediments in Norway via a thermochemolysis Py-GC–MS method (Gomiero et al., 2019). Using Raman/µ-FTIR spectroscopy or fluorescence microscopy, greater number counts were observed of smaller plastic particles in coastal river sediment (Klein et al., 2015; Wang et al., 2018) and seawater samples (Enders et al., 2015), confirming the qualitative trend of increasing microplastics abundance (in counts or mass) with decreasing size. Interestingly, in ocean water, the number densities of natural colloids, comprised of inorganic solids and biomass, are known to trend inversely with the particle size via well-defined power laws, but the distribution of mass of natural colloids across different size ranges are considered relatively uniform (McCave, 1984; Morel and Hering, 1993). Although the limited data on microplastics mass concentrations available thus far prevents extensive generalization, the finding that a greater mass of plastics is present with decreasing particle size favors the hypothesis that plastics are more prone to fragmentation than mineral or biological particles. This observation underscores the advantage of characterizing plastic pollution by combining sample size fractionation with a thermal analysis method such as Py-GC–MS. This approach can capture particles in minute sizes (>1.2 µm in this study, and the lower size limit was determined by sample processing method rather than thermal analysis itself). The mass of plastics observed in the fine fraction suggests that the tiny plastic debris are likely present at very high counts. Assuming a perfect spherical shape, a uniform size of 100 µm, and a density of 1.35 g/cm^3 for PET (Andrady, 2017), a sample containing 1 mg/kg of PET would have over 1000 of PET particles per kg of the sample, and the number count will be over a million for 10-µm particles. Considering this, optical or IR/Raman microscopic methods are valuable for characterizing the size, shape, and appearance of individual debris, whereas thermal analytical techniques such as Py-GC–MS offer an efficient and reliable approach to obtain aggregate mass concentration data. The two groups of methods are therefore complementary to one another (Ivleva, 2021; Qiu et al., 2016). Regardless of the choice of analysis methods, sample pretreatment is critical for eliminating background materials in the samples, and rigorous QA/QC protocols are needed to avoid contamination during pretreatment and analysis.

Aside from the debris size, sampling depth also casts a strong influence on the mass concentration of plastics. The effect of sampling depth manifests differently in the fine and intermediate size fractions. Fine PET and PS debris are more abundant in the surface 0–5 cm layer (Figs. 3a and 4a). In contrast, among the intermediate-sized solids, PET seems to be more enriched with increasing sample depth, while PS has no clear distribution pattern across the depth (Fig. 3b and 4b). The detection of significantly higher quantities of fine particles of PET and PS in the 0–5 cm surface sample is consistent with the understanding that beach surface is an important venue for degradation and fragmentation of primary plastic debris (Andrady, 2017; Halle et al., 2016; Song et al., 2017). Macro-debris released from anthropogenic sources and brought to the beach by water and air movement may break down into finer pieces on the beach surface due to exposure to the sunlight (UV) and mechanical ablation caused by tidal movement (Song et al., 2017). In the natural environment, UV exposure initiates polymer degradation, leading to surface oxidation, polymer chain scission, and change in crystallinity (Andrady, 2017). Over time, this results in fracture formation and chipping of small particles away from the surface (Lambert and Wagner, 2016). Another factor that may contribute to an elevated level of fine debris in the surface relates to the deposition of small light particles carried by wind or tidal currents. To understand the relative importance of the various sources of microplastics, extending this size- and depth-dependent analysis of plastics to seawater and terrestrial soil will be valuable, which is a subject of ongoing efforts.

The distributions of PET and PS across the sampling depth suggests the nature of the plastics including their physical and chemical properties influences their degradation pathways. PET is predominantly used in consumer packaging, including food and beverage bottles, and as polyesters in synthetic clothing. PET undergoes photo-oxidation upon exposure to UV and hydrolytic degradation in the presence of humidity or water. PET weathering is accelerated when there is concerted actions of solar irradiation, water exposure, temperature cycling, and mechanical agitation, such as in the surface beach environment (Gok et al., 2019). Lab simulated aging study confirms that the combined effect of UV exposure and mechanical stress promotes PET degradation (An et al., 2023). This seems to explain the observations that PET exists predominantly as fine particles (1.2 µm–100 µm) in the surface sand at both beaches, whereas larger PET particles in the intermediate size fraction is more abundant in the subsurface due to limited exposure to sunlight and tidal influence. Aside from a weathering effect, fine PET particles may be released from synthetic textile. PS, particularly in the form of expanded foam, is used widely in food packaging and as cushion peanuts in the shipping industry (Andrady, 2011). Studies have shown that PS is more prone to fragmentation during environmental weathering than polyolefins (Lambert and Wagner, 2016; Song et al., 2017; Weinstein et al., 2016). In the case of expanded PS (EPS), creation of thin layers in a foam structure further weakens its mechanical strength, thus mechanical agitation alone without solar exposure can induce significant fragmentation (Song et al., 2017). The prevalent presence of PS as fine particles in most samples, except for 5–10 cm at Hampton beach, supports its susceptibility to fragmentation.

The effect of sampling depth on microplastic distribution has been investigated in recent studies at beaches in the Mediterranean region (La Nasa et al., 2020; Piperagkas et al., 2019). In one study using FTIR

microscopy, more plastic debris in the form of fragments were present in the samples collected at a depth of 15 cm than in surface samples, while microfibers were more abundant on the surface (Piperagkas et al., 2019). As different methods were used to quantify microplastics, the findings of the prior study are not directly comparable to our results. Nonetheless, based on the categorization criteria, microfibers of the prior study fall into the fine size fraction of this study, whereas fragments correspond more closely to our intermediate or coarse fractions. In another study, the highest amount of PS was detected in the surface sand than at a depth of 15 cm and 35 cm based on DCM extraction and Py-GC–MS (La Nasa et al., 2020). Considering these studies, the depth-dependent distribution of microplastics at the Mediterranean beaches is in line with the findings of the present study. That being said, there is inherently high variability in surface sampling due to small light debris being moved easily with air flow and currents. In comparison, subsurface samples from a sufficient depth, greater than the depth range explored in this study, may offer more representative info on microplastics accumulation in the sediments over a long period.

The amount of microplastics present on beaches are affected by its proximity to urban centers, beach-visiting traffic, local industry and aquacultural activities, and municipal waste management practices (Retama et al., 2016; Wessel et al., 2016). A recent survey of three different beaches in India found that the highest level of microplastics was present at a beach close to a megacity with the highest anthropogenic activities compared to beaches near an industrial city or a tourist spot (Tiwari et al., 2019). Aside from human influence, the local waves and currents, topography of the chosen transects, geographical characteristics, storm activity are significant factors that influence the pattern of distribution of microplastics (Brander et al., 2020). The two beaches studied here have similar natural settings due to their proximity to each other, however, Hampton Beach, with its well-developed tourism establishment surrounding the beach, bears a higher volume of visitors than the neighboring Salisbury Beach on a natural reserve. Interestingly, we did not see a significant difference in microplastic mass concentrations at the two beaches. Discussion with the seacoast regional officer suggests that there was frequent mechanical raking (3 times per week May through August) in addition to biweekly volunteer cleaning events at Hampton beach. The swift removal of macro-debris by these efforts may possibly serve to alleviate the impact of anthropogenic activities on microplastic generation on a beach.

4. Conclusion

In this study, a method combining low-temperature solvation extraction and Py-GC–MS for quantitative analysis of PET, PS, PVC, and PA-66 in beach sand was demonstrated. 2-Chlorophenol was identified as the optimal solvent for its ability to dissolve the above polymers at room temperature, and the one-step solvent extraction simplifies sample preparation procedures and reduces interference from the background matrix. High quality calibration data and sensitive detection of PET and PS (LOQ < 0.1 μg) were achieved with this method. PE and PP were analyzed as solid particles via direct Py-GC–MS due to their limited solubility in solvents, and this approach is less sensitive and bears higher uncertainties than the solvent-extraction-Py-GC–MS method. Analysis of samples collected at two beaches along the New England coast of the U. S. indicates variance in microplastic distribution due to sample depth and particle size. Greater abundance of PET and PS was observed in the finest size fraction (1.2 μm–100 μm) than in the intermediate (100 μm–1.2 mm) size range. The fine particles of PET and PS were more enriched in the surface sand collected from the top 5-cm depth. In the intermediate fraction, more PET was detected with increasing depth with no conclusive trend for PS. The predominant presence of PET and PS as fine particles and their higher occurrence on the surface could be attributed to the continuous weathering and fragmentation of plastic debris in the beach environment in the presence of UV and mechanical ablation from tidal activities. The observed results may also be contributed by the transport of fine plastic particles from remote sources through wind and tidal movement. This study demonstrates the capability of the proposed beach sampling and sample analysis methods. Applying these methods in future research will better clarify the sources and migration patterns of microplastics in the environment.

CRediT authorship contribution statement

Mythreyi Sivaraman: Writing – original draft, Visualization, Validation, Project administration, Methodology, Investigation. **Lingfei Fan:** Investigation, Methodology. **Weile Yan:** Writing – review & editing, Supervision, Project administration, Methodology, Investigation, Funding acquisition, Conceptualization.

Declaration of competing interest

The authors declare that they have no known competing financial interests or personal relationships that could have influenced the work reported in this paper.

Data availability

Data will be made available on request.

Acknowledgements

This study is supported by the U.S. National Science Foundation (CHE-2304991). The authors wish to thank Dr. Robert Whitehouse from UML for suggestions given to the study and comments on the manuscript and Cole Radke for assistance during field sampling.

Appendix A. Supplementary data

Additional info on quantities of plastics found in Salisbury Beach and Hampton Beach; comparison of IS signals of solid and solvent extracted samples; and Py-GC-MS calibration results of PET, PS, PA-66, PVC, PE and PP. Supplementary data to this article can be found online at https://doi.org/10.1016/j.scitotenv.2024.176009.

References

Alvarez-Zeferino, J.C., Cruz-Salas, A.A., Vázquez-Morillas, A., Ojeda-Benitez, S., 2020. Method for quantifying and characterization of microplastics in sand beaches. Rev. Int. Contam. Ambie. 36 (1), 151–164.
An, Y., Kajiwara, T., Padermshoke, A., Van Nguyen, T., Feng, S., Mokudai, H., Masaki, T., Takigawa, M., Van Nguyen, T., Masunaga, H., 2023. Environmental degradation of nylon, poly (ethylene terephthalate)(PET), and poly (vinylidene fluoride)(PVDF) fishing line fibers. ACS Appl. Polym. Mater. 5 (6), 4427–4436.
Andrady, A.L., 2011. Microplastics in the marine environment. Mar. Pollut. Bull. 62 (8), 1596–1605.
Andrady, A.L., 2017. The plastic in microplastics: a review. Mar. Pollut. Bull. 119 (1), 12–22.
Becker, R., Altmann, K., Sommerfeld, T., Braun, U., 2020. Quantification of microplastics in a freshwater suspended organic matter using different thermoanalytical methods – outcome of an interlaboratory comparison. J. Anal. Appl. Pyrolysis 148, 104829.
Bergmann, M., Mützel, S., Primpke, S., Tekman, M.B., Trachsel, J., Gerdts, G., 2019. White and wonderful? Microplastics prevail in snow from the Alps to the Arctic. Sci. Adv. 5 (8), eaax1157.
Bour, A., Avio, C.G., Gorbi, S., Regoli, F., Hylland, K., 2018. Presence of microplastics in benthic and epibenthic organisms: influence of habitat, feeding mode and trophic level. Environ. Pollut. 243 (Pt B), 1217–1225.
Brander, S.M., Renick, V.C., Foley, M.M., Steele, C., Woo, M., Lusher, A., Carr, S., Helm, P., Box, C., Cherniak, S., 2020. Sampling and quality assurance and quality control: a guide for scientists investigating the occurrence of microplastics across matrices. Appl. Spectrosc. 74 (9), 1099–1125.
Browne, M.A., Galloway, T.S., Thompson, R.C., 2010. Spatial patterns of plastic debris along estuarine shorelines. Environ. Sci. Technol. 44 (9), 3404–3409.
Browne, M.A., Crump, P., Niven, S.J., Teuten, E., Tonkin, A., Galloway, T., Thompson, R., 2011. Accumulation of microplastic on shorelines woldwide: sources and sinks. Environ. Sci. Technol. 45 (21), 9175–9179.
Castelvetro, V., Corti, A., Biale, G., Ceccarini, A., Degano, I., La Nasa, J., Lomonaco, T., Manariti, A., Manco, E., Modugno, F., Vinciguerra, V., 2021. New methodologies for the detection, identification, and quantification of microplastics and their

environmental degradation by-products. Environ. Sci. Pollut. Res. 28 (34), 46764–46780.
Ceccarini, A., Corti, A., Erba, F., Modugno, F., La Nasa, J., Bianchi, S., Castelvetro, V., 2018. The hidden microplastics: new insights and figures from the thorough separation and characterization of microplastics and of their degradation byproducts in coastal sediments. Environ. Sci. Technol. 52 (10), 5634–5643.
Chamas, A., Moon, H., Zheng, J., Qiu, Y., Tabassum, T., Jang, J.H., Abu-Omar, M., Scott, S.L., Suh, S., 2020. Degradation rates of plastics in the environment. ACS Sustain. Chem. Eng. 8 (9), 3494–3511.
Cheshire, A., Adler, E., 2009. UNEP/IOC Guidelines on Survey and Monitoring of Marine Litter.
Conley, K., Clum, A., Deepe, J., Lane, H., Beckingham, B., 2019. Wastewater treatment plants as a source of microplastics to an urban estuary: removal efficiencies and loading per capita over one year. Water Res. X 3, 100030.
Coppock, R.L., Cole, M., Lindeque, P.K., Queirós, A.M., Galloway, T.S., 2017. A small-scale, portable method for extracting microplastics from marine sediments. Environ. Pollut. 230, 829–837.
David, J., Steinmetz, Z., Kučerík, J.I., Schaumann, G.E., 2018. Quantitative analysis of poly(ethylene terephthalate) microplastics in soil via thermogravimetry–mass spectrometry. Anal. Chem. 90 (15), 8793–8799.
Dümichen, E., Eisentraut, P., Bannick, C.G., Barthel, A.-K., Senz, R., Braun, U., 2017. Fast identification of microplastics in complex environmental samples by a thermal degradation method. Chemosphere 174, 572–584.
Egger, M., Sulu-Gambari, F., Lebreton, L., 2020. First evidence of plastic fallout from the North Pacific Garbage Patch. Sci. Rep. 10 (1), 7495.
Enders, K., Lenz, R., Stedmon, C.A., Nielsen, T.G., 2015. Abundance, size and polymer composition of marine microplastics ≥10μm in the Atlantic Ocean and their modelled vertical distribution. Mar. Pollut. Bull. 100 (1), 70–81.
Fischer, M., Scholz-Böttcher, B.M., 2017. Simultaneous trace identification and quantification of common types of microplastics in environmental samples by pyrolysis-gas chromatography-mass spectrometry. Environ. Sci. Technol. 51 (9), 5052–5060.
Fischer, M., Scholz-Böttcher, B.M., 2019. Microplastics analysis in environmental samples – recent pyrolysis-gas chromatography-mass spectrometry method improvements to increase the reliability of mass-related data. Anal. Methods 11 (18), 2489–2497.
GESAMP, 2016. Souces, Fate and Effects of Microplastics in the Marine Environment: A Global Assessment.
Gewert, B., Plassmann, M.M., MacLeod, M., 2015. Pathways for degradation of plastic polymers floating in the marine environment. Environ Sci Process Impacts 17 (9), 1513–1521.
Gok, A., Fagerholm, C.L., French, R.H., Bruckman, L.S., 2019. Temporal evolution and pathway models of poly (ethylene-terephthalate) degradation under multi-factor accelerated weathering exposures. PLoS One 14 (2), e0212258.
Gomiero, A., Øysæd, K.B., Agustsson, T., van Hoytema, N., van Thiel, T., Grati, F., 2019. First record of characterization, concentration and distribution of microplastics in coastal sediments of an urban fjord in south west Norway using a thermal degradation method. Chemosphere 227, 705–714.
Hale, R.C., Seeley, M.E., La Guardia, M.J., Mai, L., Zeng, E.Y., 2020. A global perspective on microplastics. J. Geophys. Res. Oceans 125 (1).
Halle, A.T., Ladirat, L., Gendre, X., Goudouneche, D., Pusineri, C., Routaboul, C., Tenailleau, C., Duployer, B., Perez, E., 2016. Understanding the fragmentation pattern of marine plastic debris. Environ. Sci. Technol. 50 (11), 5668–5675.
Ivleva, N.P., 2021. Chemical analysis of microplastics and nanoplastics: challenges, advanced methods, and perspectives. Chem. Rev. 121 (19), 11886–11936.
Kane, I.A., Clare, M.A., Miramontes, E., Wogelius, R., Rothwell, J.J., Garreau, P., Pohl, F., 2020. Seafloor microplastic hotspots controlled by deep-sea circulation. Science 368 (6495), 1140–1145.
Käppler, A., Fischer, M., Scholz-Böttcher, B.M., Oberbeckmann, S., Labrenz, M., Fischer, D., Eichhorn, K.-J., Voit, B., 2018. Comparison of μ-ATR-FTIR spectroscopy and py-GCMS as identification tools for microplastic particles and fibers isolated from river sediments. Anal. Bioanal. Chem. 410 (21), 5313–5327.
Klein, S., Worch, E., Knepper, T.P., 2015. Occurrence and spatial distribution of microplastics in river shore sediments of the Rhine-Main area in Germany. Environ. Sci. Technol. 49 (10), 6070–6076.
La Nasa, J., Biale, G., Mattonai, M., Modugno, F., 2020. Microwave-assisted solvent extraction and double-shot analytical pyrolysis for the quali-quantitation of plasticizers and microplastics in beach sand samples. J. Hazard. Mater. 401, 123287.
Lambert, S., Wagner, M., 2016. Formation of microscopic particles during the degradation of different polymers. Chemosphere 161, 510–517.
Lauschke, T., Dierkes, G., Schweyen, P., Ternes, T.A., 2021. Evaluation of poly(styrene-d5) and poly(4-fluorostyrene) as internal standards for microplastics quantification by thermoanalytical methods. J. Anal. Appl. Pyrolysis 159, 105310.
Lebreton, L.C.M., van der Zwet, J., Damsteeg, J.-W., Slat, B., Andrady, A., Reisser, J., 2017. River plastic emissions to the world's oceans. Nat. Commun. 8 (1), 15611.
Lebreton, L., Egger, M., Slat, B., 2019. A global mass budget for positively buoyant macroplastic debris in the ocean. Sci. Rep. 9 (1), 12922.
Li, D., Liu, K., Li, C., Peng, G., Andrady, A.L., Wu, T., Zhang, Z., Wang, X., Song, Z., Zong, C., Zhang, F., Wei, N., Bai, M., Zhu, L., Xu, J., Wu, H., Wang, L., Chang, S., Zhu, W., 2020. Profiling the vertical transport of microplastics in the West Pacific Ocean and the East Indian Ocean with a novel in situ filtration technique. Environ. Sci. Technol. 54 (20), 12979–12988.
Lippiatt, S., Opfer, S., Arthur, C., 2013. Marine Debris Monitoring and Assessment: Recommendations for Monitoring Debris Trends in the Marine Environment.
Masura, J., Baker, J., Foster, G., Arther, C., Herring, C., 2015. Laboratory methods for the analysis of microplastics in the marine environment: recommendations for quantifying synthetic particles in waters and sediments. In: NOAA Technical Memorandum NOS-OR&R-48.
Matsueda, M., Mattonai, M., Iwai, I., Watanabe, A., Teramae, N., Robberson, W., Ohtani, H., Kim, Y.-M., Watanabe, C., 2021. Preparation and test of a reference mixture of eleven polymers with deactivated inorganic diluent for microplastics analysis by pyrolysis-GC–MS. J. Anal. Appl. Pyrolysis 154, 104993.
McCave, I.N., 1984. Size spectra and aggregation of suspended particles in the deep ocean. Deep Sea Res. A Oceanogr. Res. Pap. 31 (4), 329–352.
Morel, F.M.M., Hering, J.G., 1993. Principles and Applications of Aquatic Chemistry. Wiley, New York.
Murphy, F., Ewins, C., Carbonnier, F., Quinn, B., 2016. Wastewater treatment works (WwTW) as a source of microplastics in the aquatic environment. Environ. Sci. Technol. 50 (11), 5800–5808.
Okoffo, E.D., Ribeiro, F., O'Brien, J.W., O'Brien, S., Tscharke, B.J., Gallen, M., Samanipour, S., Mueller, J.F., Thomas, K.V., 2020. Identification and quantification of selected plastics in biosolids by pressurized liquid extraction combined with double-shot pyrolysis gas chromatography–mass spectrometry. Sci. Total Environ. 715, 136924.
Peñalver, R., Arroyo-Manzanares, N., López-García, I., Hernández-Córdoba, M., 2019. An overview of microplastics characterization by thermal analysis. Chemosphere 242, 125170.
Piperagkas, O., Papageorgiou, N., Karakassis, I., 2019. Qualitative and quantitative assessment of microplastics in three sandy Mediterranean beaches, including different methodological approaches. Estuar. Coast. Shelf Sci. 219, 169–175.
Qiu, Q., Tan, Z., Wang, J., Peng, J., Li, M., Zhan, Z., 2016. Extraction, enumeration and identification methods for monitoring microplastics in the environment. Estuar. Coast. Shelf Sci. 176, 102–109.
Quinn, B., Murphy, F., Ewins, C., 2017. Validation of density separation for the rapid recovery of microplastics from sediment. Anal. Methods 9 (9), 1491–1498.
Ramos, M.A.V., Yan, W., Li, X.Q., Koel, B.E., Zhang, W.X., 2009. Simultaneous oxidation and reduction of arsenic by zero-valent iron nanoparticles: understanding the significance of the core-shell structure. J. Phys. Chem. C 113 (33), 14591–14594.
Retama, I., Jonathan, M., Shruti, V., Velumani, S., Sarkar, S., Roy, P.D., Rodríguez-Espinosa, P., 2016. Microplastics in tourist beaches of Huatulco Bay, Pacific coast of southern Mexico. Mar. Pollut. Bull. 113 (1–2), 530–535.
Seeley, M.E., Lynch, J.M., 2023. Previous successes and untapped potential of pyrolysis–GC/MS for the analysis of plastic pollution. Anal. Bioanal. Chem. 415 (15), 2873–2890.
Simon, M., van Alst, N., Vollertsen, J., 2018. Quantification of microplastic mass and removal rates at wastewater treatment plants applying Focal Plane Array (FPA)-based Fourier Transform Infrared (FT-IR) imaging. Water Res. 142, 1–9.
Sluka, R., Calcutt, J., Nussbaumer, A., 2018. Guidelines for sampling microplastics on sandy beaches. In: A Rocha International's and Coastal Conservation, pp. 1–41.
Song, Y.K., Hong, S.H., Jang, M., Han, G.M., Jung, S.W., Shim, W.J., 2017. Combined effects of UV exposure duration and mechanical abrasion on microplastic fragmentation by polymer type. Environ. Sci. Technol. 51 (8), 4368–4376.
Steinmetz, Z., Kintzi, A., Muñoz, K., Schaumann, G.E., 2020. A simple method for the selective quantification of polyethylene, polypropylene, and polystyrene plastic debris in soil by pyrolysis-gas chromatography/mass spectrometry. J. Anal. Appl. Pyrolysis 147, 104803.
Sun, J., Dai, X.H., Wang, Q.L., van Loosdrecht, M.C.M., Ni, B.J., 2019. Microplastics in wastewater treatment plants: detection, occurrence and removal. Water Res. 152, 21–37.
Thompson, R.C., Olsen, Y., Mitchell, R.P., Davis, A., Rowland, S.J., John, A.W., McGonigle, D., Russell, A.E., 2004. Lost at sea: where is all the plastic? Science 304 (5672), 838.
Tiwari, M., Rathod, T., Ajmal, P., Bhangare, R., Sahu, S., 2019. Distribution and characterization of microplastics in beach sand from three different Indian coastal environments. Mar. Pollut. Bull. 140, 262–273.
Wang, Z., Su, B., Xu, X., Di, D., Huang, H., Mei, K., Dahlgren, R.A., Zhang, M., Shang, X., 2018. Preferential accumulation of small (<300 μm) microplastics in the sediments of a coastal plain river network in eastern China. Water Res. 144, 393–401.
Weinstein, J.E., Crocker, B.K., Gray, A.D., 2016. From macroplastic to microplastic: degradation of high-density polyethylene, polypropylene, and polystyrene in a salt marsh habitat. Environ. Toxicol. Chem. 35 (7), 1632–1640.
Wessel, C.C., Lockridge, G.R., Battiste, D., Cebrian, J., 2016. Abundance and characteristics of microplastics in beach sediments: insights into microplastic accumulation in northern Gulf of Mexico estuaries. Mar. Pollut. Bull. 109 (1), 178–183.
Zhou, X.-X., Hao, L.-T., Wang, H.-Y.-Z., Li, Y.-J., Liu, J.-F., 2019. Cloud-point extraction combined with thermal degradation for nanoplastic analysis using pyrolysis gas chromatography-mass spectrometry. Anal. Chem. 91 (3), 1785–1790.